Carbohydrate Polymers 96 (2013) 602–610

Contents lists available at SciVerse ScienceDirect

Carbohydrate Polymers

journal homepage: www.elsevier.com/locate/carbpol

Characterization of starch films containing starch nanoparticles. Part 2: Viscoelasticity and creep properties

Ai-min Shi[a,1], Li-jun Wang[b,1], Dong Li[a,*], Benu Adhikari[c]

[a] College of Engineering, China Agricultural University, P.O. Box 50, 17 Qinghua Donglu, Beijing 100083, China
[b] College of Food Science and Nutritional Engineering, China Agricultural University, Beijing, China
[c] School of Health Sciences, University of Ballarat, VIC 3353, Australia

ARTICLE INFO

Article history:
Received 11 September 2012
Received in revised form 9 October 2012
Accepted 21 October 2012
Available online 1 November 2012

Keywords:
Corn starch film
Starch nanoparticles
Frequency sweep
Creep-recovery behavior
Time–temperature superposition (TTS)

ABSTRACT

Starch films were successfully produced by incorporating spray dried and vacuum-freeze dried starch nanoparticles. The frequency sweep, creep-recovery behavior and time–temperature superposition (TTS) on these films were studied. All these films exhibited dominant elastic behavior (than viscous behavior) over the entire frequency range (0.1–100 rad/s). The incorporation of both types of starch nanoparticles increased the storage and loss modulus, tan δ, creep strain, creep compliance and creep rate at long time frame and reduced the recovery rate of films while the effect of different kinds of starch nanoparticles on these parameters was similar both in magnitude and trend. TTS method was successfully used to predict long time (over 20 days) creep behavior through the master curves. The addition of these nanoparticles could increase the activation energy parameter used in TTS master curves. Power law and Burger's models were capable of fitting storage and loss modulus ($R^2 > 0.79$) and creep data ($R^2 > 0.96$), respectively.

1. Introduction

Starch-based edible films or non-edible packaging films contribute toward the protection of environment due to their biodegradability (Ryu, Rhim, Roh, & Kim, 2002). The current and potential applications of starch-based films in food (Laohakunjit & Noomhorm, 2004), medicine (Krogars, Heinämäki, Antikainen, Karjalainen, & Yliruusi, 2003) and packaging industry (Avella et al., 2005) have been adequately highlighted.

The starch or starch-based films can be produced by a number of ways and the solution casting method is commonly used in research and development stage (Dawson, Hirt, Rieck, Acton, & Sotthibandhu, 2003; Kampeerapappun, Aht-ong, Pentrakoon, & Srikulkit, 2007; Obara & McGinity, 1994). The properties of films, to a greater extent, are determined by the composition of film forming solution. Materials such as gelatin (Veiga-Santos, Oliveira, Cereda, & Scamparini, 2007), cellulose (Wittaya, 2009), chitosan (Xu, Kim, Hanna, & Nag, 2005) and plasticizers such as glycerol (Alves, Mali, Beléia, & Grossmann, 2007), xylitol (Talja, 2007) and their combination (Muscat, Adhikari, Adhikari, & Chaudhary, 2012) are used to improve the physicochemical and mechanical properties of starch-based films. In addition, the starch or starch-based films can also be modified by the addition of nanoparticles (Wu, Wang, & Ge, 2009).

Starch nanoparticles are nano-sized (1–1000 nm) particulates of starch prepared by chemically cross-linking starch molecules with appropriate cross-linkers. In our pervious study, we reported that the starch nanoparticle can be successfully prepared through water-in-oil (w/o) mini-emulsion cross-linking technique using high pressure homogenizer (Shi, Li, Wang, Li, & Adhikari, 2011). As both the starch-based films and starch nanoparticles have the same material (starch) as the major component, it is interesting to investigate the effect of presence/incorporation of starch nanoparticles on the properties of starch-based films.

Viscoelastic properties are important indicators which allow prediction of time-dependent deformation of polymeric substances in films and solutions exposed to various environmental conditions such as heat and stress/strain (Chen & Lai, 2008; Famá, Rojas, Goyanes, & Gerschenson, 2005; Kim et al., 2009). In addition, viscoelastic properties such as frequency-dependence and creep-recovery behavior can also be affected by the composition of polymeric substances.

Mendieta-Taboada, Sobral, Carvalho, and Habitante (2008) studied the frequency sweep tests in the range from 0.01 to 200 Hz in films produced from poly(vinyl alcohol) (PVA)-gelatin blends containing 10–40% PVA. They found that modulus of elasticity increased with increase in PVA concentration between 10% and 30% of PVA. Alvarez, Kenny, and Vázquez (2004) reported that the addition of sisal fibers in biodegradable cellulose derivatives/starch

* Corresponding author. Tel.: +86 10 62737351; fax: +86 10 62737351.
E-mail address: dongli@cau.edu.cn (D. Li).
[1] These authors contributed equally to this work.

0144-8617/$ – see front matter © 2012 Elsevier Ltd. All rights reserved.
http://dx.doi.org/10.1016/j.carbpol.2012.10.064

Nomenclature

a_T	shift factor
E_a	activation energy (kJ/mol)
E_K	modulus of the Kelvin spring (MPa)
E_M	modulus of the Maxwell spring (MPa)
G'	storage modulus (Pa)
G''	loss modulus (Pa)
J	creep compliance ($\mu m^2/N$)
K'	index ($Pa\,s^n$)
K''	index ($Pa\,s^n$)
n'	frequency exponent
n''	frequency exponent
R	universal gas constant ($J\,K^{-1}\,mol^{-1}$)
R^2	correlation coefficient
T_0	reference temperature (K)
T	absolute temperature (K)
τ	retardation time (s)
t	loading time (s)
η_M	viscosity of the Maxwell dashpot (MPa s)
η_K	viscosity of the Kelvin dashpot (MPa s)
ω	angle frequency (rad/s)
$\tan\delta$	tangent of loss angle
ε	strain of suspension
ε'	creep rate (s^{-1})
σ_0	constantly applied compressive stress (MPa)

composite films significantly improved the creep resistance in cellulose derivatives/starch composite films. Bonacucina et al. (2006) investigated the effect of different plasticizers on the creep behavior of pregelatinised starch acetate (Amprac 01) free standing films and reported that the addition of plasticizers enhanced the creep compliance.

We recently developed starch-based films which incorporated starch nanoparticles. The physical characteristics such as amorphous crystalline/nature, glass transition behavior and temperature dependence of strain of those starch nanoparticles containing films were studied. However, the effects of incorporation of starch nanoparticles on the frequency sweep and creep-recovery behaviors of starch-based films are not reported previously. As the understanding of the frequency dependence of viscoelastic and creep-recovery behaviors of starch film is important, we are reporting these behaviors in this manuscript.

The experimental time frame affects the creep behavior and the short-time and long-time creep strain and creep compliance are quite different. However, long-term creep behavior is not easy to be measured due to limitations in instrument as well as in the material. In this regard, the time–temperature superposition (TTS) is one of the most important methods which could predict the long-time creep using the short-term creep values obtained at higher or lower temperatures (Shaito, 2008; Urzhumtsev, 1975; Weick, 2006). The TTS is commonly used to study the long-term creep of polymeric films (Chevali, Dean, & Janowski, 2010; Patra, Salerno, Diaspro, & Athanassiou, 2011; Xu, Wu, Lei, & Yao, 2010). However, the application of TTS for the prediction of long-term creep in starch films with and without starch nanoparticles is not reported.

Therefore, we aimed at investigating the frequency sweep and creep-recovery behavior of starch films with and without starch nanoparticles. We also attempted to predict the long term-creep of starch films in the presence and absence of starch nanoparticles using TTS. The effect of addition of spray dried and vacuum freeze dried nanoparticles in the starch films was also evaluated. The modeling of the frequency dependence of elastic and loss modulus data was carried out using Power law model. Similarly, the creep strain versus time data of the films was modeled using Burger's model.

2. Materials and methods

2.1. Materials

Corn starch was obtained from Hebei Zhangjiakou Yujing Food Co. Ltd. (Hebei, China). Glycerol (analytical grade) was purchased from Beijing Chemical Reagent Ltd. (Beijing, China). Xylitol (food grade) was purchased from Tianjin Jinguigu Science & Technology Development Co. Ltd. All of these materials were used without further purification.

2.2. Preparation of starch nanoparticles

Starch nanoparticles were produced following the emulsion cross-linking method based on the emulsion cross-linking technology using a high pressure homogenizer. This method was presented in detail in our previous paper (Shi et al., 2011). Spray drying and vacuum freeze drying were used to remove the water and convert the nanoparticles in dry particulate form. Spray drying was carried out at inlet temperature of 100 °C, outlet temperature of 56 °C and feed flow rate of 5.4 mL/min. In vacuum freeze drying, the samples were frozen for 5 h at −60 °C and subsequently dried for 28 h varying the temperature from −30 °C to 45 °C. The vacuum during the freezing drying was maintained at ≤100 Pa. The details of these drying methods were also presented in our previous paper (Shi et al., 2011).

2.3. Preparation of film-forming solutions

The films were produced from the film-forming solution using a casting technique (Fu, Wang, Li, Wei, & Adhikari, 2011). Specifically, 7.0 g of pre-dried corn starch and 3.0 g of plasticizers (glycerol and xylitol, 1:1) were added into 200 mL deionized water to form starch-plasticizer dispersions. The total solid content of these dispersions was maintained at 5.0 wt.% (w/v). The dispersion batches were thoroughly stirred at 300 rpm (in beakers) for 1 h using a thermostated water bath in boiling condition. Evaporation was minimized by covering the beakers with six layers of water-resistant film. When these dispersions were fully gelatinized, they were cooled to 70 °C and 0.5 wt.% (w/v) starch nanoparticles was added. These dispersions containing starch nanoparticles were further stirred at 300 rpm for 30 min. The dispersions which did not contain the starch nanoparticles severed as the control sample.

2.4. Film casting and drying

Films were cast by syringing 8 mL of the above mentioned dispersions into 9 cm diameter polycarbonate petri dishes and then dried for over 8 h at 45 °C. These dried films were conditioned in controlled humidity chambers (25 °C, RH = 53%) until further testing. The nomenclature of these films is referenced in Table 1.

2.5. Frequency sweep tests

A dynamic mechanical analyzer (DMA, Q800, TA Instruments, New Castle, DE) was used to carry out the frequency sweep tests on all the films. The film for DMA analysis was cut into 50 mm × 10 mm strips (thickness = 0.1–0.5 mm). The film strip was then clamped to the DMA furnace at both ends and the actual gap between both ends was measured. After equilibrating at 35.00 °C for 2 min, the frequency sweep tests were performed at a frequency range of 0.1 to 100 Hz at a strain of 0.05% and a preload force of 0.01 N. Storage modulus (G'), loss modulus (G'') and $\tan\delta$ were determined

Table 1
Power law modeling parameters of frequency sweep results of starch film in the absence and presence of starch nanoparticles.[f]

Film type	Composition (except starch)	K' (Pa s^n)	n'	R^2	K'' (Pa s^n)	n''	R^2
B Film	Control sample	1243.463 ± 25.008[a]	0.091 ± 0.007[a]	0.798	94.258 ± 1.928[a]	0.096 ± 0.007[a]	0.791
S Film	Spray dried starch nanoparticles	1559.477 ± 33.437[b]	0.095 ± 0.008[a]	0.797	160.293 ± 2.842[b]	0.111 ± 0.006[a]	0.881
F Film	Vacuum Freeze dried starch nanoparticles	1907.786 ± 34.806[c]	0.094 ± 0.007[a]	0.836	184.005 ± 2.785[c]	0.116 ± 0.005[a]	0.918

[f] Values represent the mean ± standard deviation of triplicate tests. Values in a column with different superscripts were significantly different ($p < 0.05$).

and plotted against the frequency. All of these measurements were carried out in triplicate and the average values were reported.

2.6. Creep-recovery tests

The creep-recovery behavior of the starch films with or without incorporation of starch nanoparticles was determined using a dynamic mechanical analyzer (DMA, Q800, TA Instruments, New Castle, USA). The films used in these DMA tests were cut into 50 mm × 10 mm strips (thickness, 0.1–0.5 mm). The film strip was then clamped to the DMA furnace at both ends and the actual gap between both ends was measured with a small preload force of 0.001 N. After equilibrating at 35 °C for 2 min, the film samples were pressurized using a stress of 2 MPa for 5 min and then were recovered for 5 min by removing the stress. The strain and creep compliance $J(t)$ were recorded.

2.7. Time–temperature superposition (TTS)

Time–temperature superposition (TTS) was used to predict long-term creep deformation of the starch films in the presence and absence of starch nanoparticles from the accelerated testing data at different temperatures and the master curves were constructed (Xu, 2009). Specifically, starch films (50 mm × 10 mm × 0.1–0.5 mm) with and without starch nanoparticles were clamped into the DMA furnace at both ends and the actual gap between both ends was measured with a small preload force of 0.001 N. After equilibrated at each test temperature (30 °C, 50 °C, 70 °C, and 90 °C) for 2 min, the creep tests were conducted on the film samples at a stress of 2 MPa for 5 min. The creep data of strain versus time at different temperatures were recorded and plotted.

The master curve was generated by shifting the above creep curves obtained at different temperatures (30 °C, 50 °C, 70 °C, and 90 °C) horizontally along the logarithmic time axis. The shifting factor was calculated using the Arrhenius equation [Eq. (1)] (Xu, 2009).

$$\log\ a_T = \frac{E_a}{R}\left(\frac{1}{T} - \frac{1}{T_0}\right) \quad (1)$$

where E_a (kJ/mol) represents the activation energy, R ($JK^{-1}\,mol^{-1}$) is the universal gas constant, T_0 is the reference temperature (K), and T is the temperature at which the test is performed (K). Regression analysis was performed on the experimental data to fit Eq. (1). The statistical package SPSS was used to determine the activation energy (E_a) and the associated correlation coefficient (R^2) was also determined. Master curves of creep strain *versus* time of all the tested films were prepared for a long time scale (over 20 days). 90 °C was used as the reference temperature (T_f) for this purpose.

2.8. Statistical analysis

All of these rheological measurements were carried out in triplicate. The experimental rheological data were obtained directly from the Universal Analysis 2000 data analysis software (TA Instruments Ltd., New Castle, DE). The averaged value of triplicate runs was reported along with the standard deviation.

Duncan's multiple comparison method was used to determine the significance using the SAS software (SAS Institute Inc., Cary, NC, USA). A confidence level was set at $P < 0.05$.

3. Results and discussion

3.1. Morphology of the films

The morphology of three starch films (films containing spray and vacuum freeze dried starch nanoparticles and the control) and starch nanoparticles obtained through SEM are presented in Fig. 1. As can be seen from this figure, the surface of starch film in the absence of starch nanoparticles is smooth perhaps due to plasticization effect of glycerol. The surface morphology of the starch films containing starch nanoparticles (Fig. 1B and C) shows greater roughness due to the presence of many protuberances or particles. Based on the size and morphology of starch nanoparticles in Fig. 1D and E, it can be reasoned that these protuberances are resulted from the presence of starch nanoparticles because the only difference in these films is the presence or absence of starch nanoparticles. It can also be seen from Fig. 1 (panel B and C) that the method of preparation of the starch nanoparticles (spray drying or vacuum freeze drying) does not seem to introduce discernible difference in the surface morphology of the starch films.

3.2. Analysis of frequency sweep tests

Fig. 2 shows the frequency dependence of storage modulus (G'), loss modulus (G'') and $\tan\delta$ of starch film with and without starch nanoparticles. As can be seen from this figure, the storage modulus values of all the films are higher than the corresponding values of loss modulus over the entire frequency range studied (0.1–100 rad/s). These observations suggest that these corn starch films exhibit dominant elastic behavior (than viscous behavior) whether or not the starch nanoparticles are present (Cespi, Bonacucina, Mencarelli, Casettari, & Palmieri, 2011). In all of these films, the storage and loss modulus increase slowly and $\tan\delta$ varies slightly when the angular frequency increases. The very weak frequency dependence of G', G'' and $\tan\delta$ in these films suggests that these films have glassy consistency (Cespi et al., 2011). It can also be seen from Fig. 2 that the addition of starch nanoparticles in starch film results into the increase in storage modulus, loss modulus and $\tan\delta$ quite significantly ($P < 0.05$) over the entire frequency range studied (0.1–100 rad/s). However, at the same frequency range (0.1–100 rad/s), the starch nanoparticles obtained from spray and vacuum freeze drying methods do not show significant ($P > 0.05$) difference in loss modulus and $\tan\delta$ although the storage modulus is significantly ($P < 0.05$) affected. The starch film containing vacuum freeze dried starch nanoparticles has higher value of storage modulus compared to the films containing spray dried starch nanoparticles over the entire frequency range studied. Amongst the films tested, the film containing spray dried starch nanoparticles shows the highest value of $\tan\delta$. This illustrates that the presence of starch nanoparticles in starch films can enhance both the elastic and viscous behavior. The increase of $\tan\delta$ suggests that the viscous component is affected to a greater extent (than the elastic component) when the nanoparticles are incorporated in starch

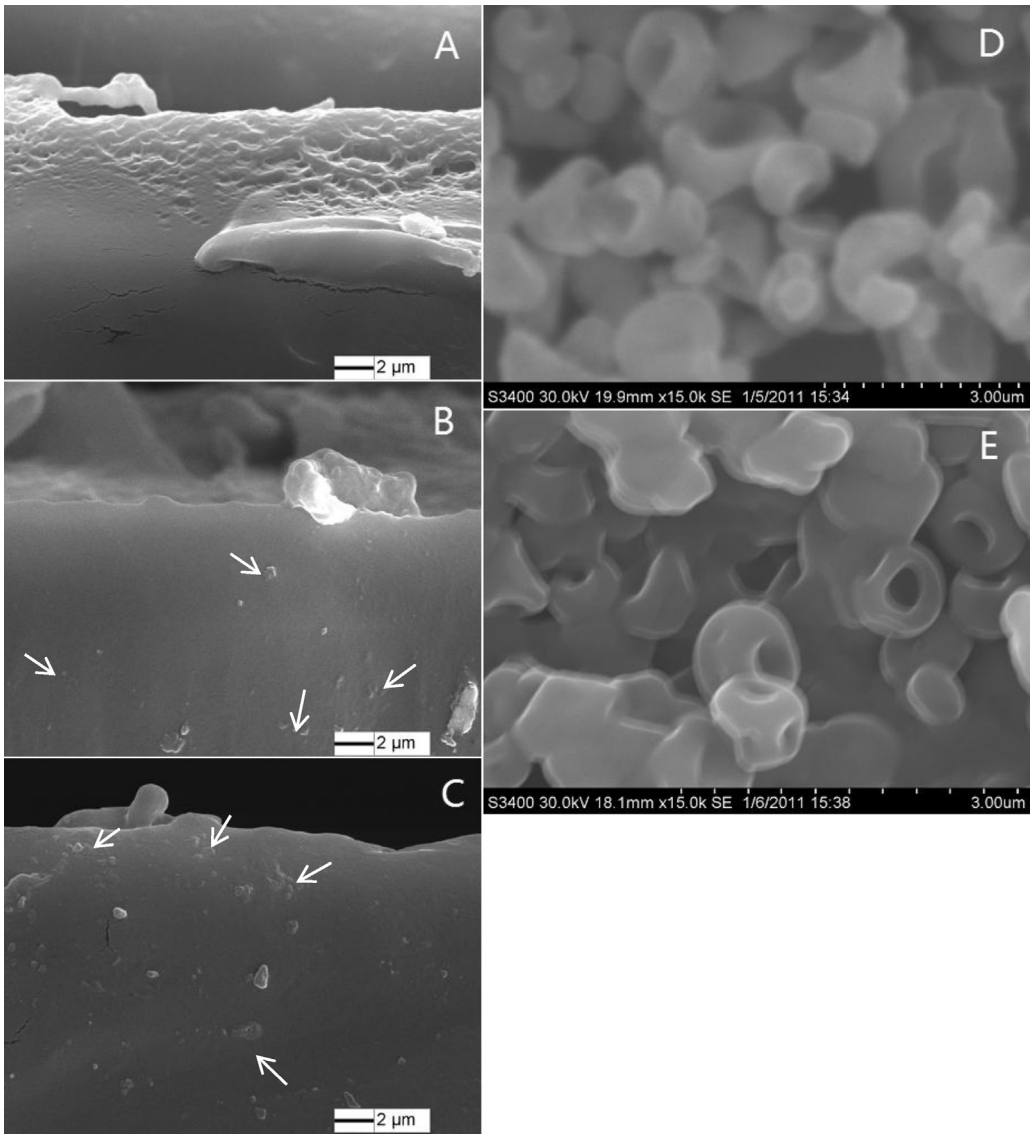

Fig. 1. SEM microphotographs of starch nanoparticles and starch films with or without starch nanoparticles. Panel A represents B film; panel B represents S film; panel C represents F film; panel D represents spray dried starch nanoparticles; and panel E represents vacuum freeze dried starch nanoparticles.

films suggesting that the films containing nanoparticles will have higher flexibility compared to the starch-alone (control) films. This might be due to the fact that the starch nanoparticles could fill the possible voids or free spaces in the structure of the film and also serve as lubricating agent (Wu et al., 2009). Starch nanoparticles have higher rigidity compared to the common plasticizers (such as glycerol and xylitol), and hence, the presence of these nanoparticles can result into films with higher strength (storage modulus). At the same time the starch nanoparticles have similar hydrophilic groups as in starch molecules which can potentially increase the number of intermolecular hydrogen bonds (loss modulus). The integral effect of the above mutually opposing phenomena is that the increase or variation in $\tan\delta$ is quite small and steady which resulted into small increase in loss and storage modulus within the frequency range tested (1–100 rad/s).

Power law models represented by Eqs. (2) and (3) were used to analyze the frequency dependence of G' and G'' (Tselev et al., 2004).

$$G' = K' \cdot \omega^{n'} \quad (2)$$

$$G'' = K'' \cdot \omega^{n''} \quad (3)$$

where K' and K'' are Power law constants and reflect the elastic and viscous properties, respectively. n' and n'' are referred to as the frequency exponents and ω is the angular frequency (rad/s).

The Power law parameters of G' and G'' for these suspensions are presented in Table 1. As can be seen from this table, the regression coefficients of G' and G'' are around 0.79–0.91 which suggests that the Power law model can basically represent the experimental G' and G'' data. The K' values of all these films are higher than the K'' values (at the same angular frequency), indicating that the starch film with and without starch nanoparticles displays higher elastic effect than viscous effect within the frequency range of 0.1–100 rad/s (Cespi et al., 2011). This observation corroborates well with the fact that the $\tan\delta$ of all the film were always very low (0.05–0.25). Furthermore, the starch films containing starch nanoparticles have higher K' and K'' values compared to the starch-only control film which is also in accord with the results presented in Fig. 2. The films containing the starch nanoparticles have higher storage and loss modulus values than those of the starch-only film. The starch film containing vacuum freeze dried starch nanoparticles exhibits higher K' and K'' values compared to that of the film containing spray dried starch nanoparticles which agrees with

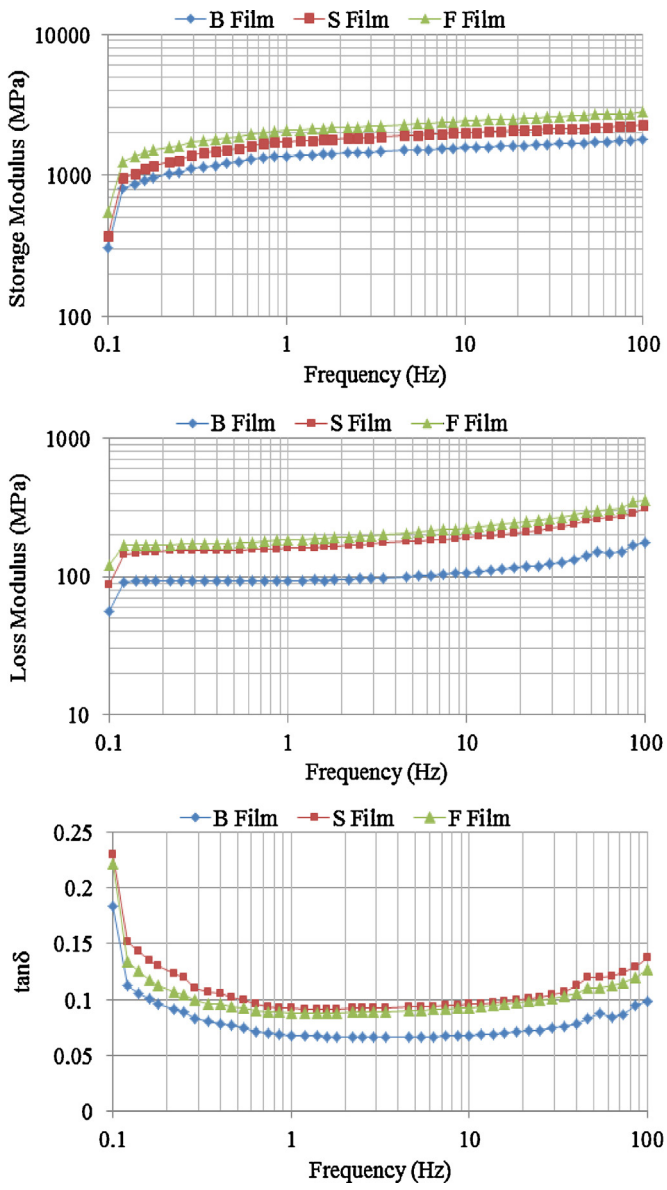

Fig. 2. The variation of (A) storage modulus, (B) loss modulus and (C) tan δ with angular frequency of the starch films in the absence or presence of starch nanoparticles.

the data presented in Fig. 2. These observations suggest that the presence of starch nanoparticles can enhance both the elastic and viscous components of starch film while the vacuum freeze dried starch nanoparticles bring about the greater impact. The n' and n'' values of all the films are close and the difference is statistically insignificant ($P > 0.05$). These observations indicate that these starch films in the presence or absence of these nanoparticles have similar frequency sensitivity.

3.3. Analysis of creep-recovery behavior

The creep-recovery behavior of starch films in the absence and presence of starch nanoparticles is presented in Fig. 3. As can be seen from Fig. 3A, creep behavior of the films in the absence and presence of the nanoparticles is quite different. Starch films containing nanoparticles (irrespective of drying methods used) show significantly higher strain values compared to that of the starch-only (control) film over the entire creep and recovery time frame. These results further support the earlier observations that

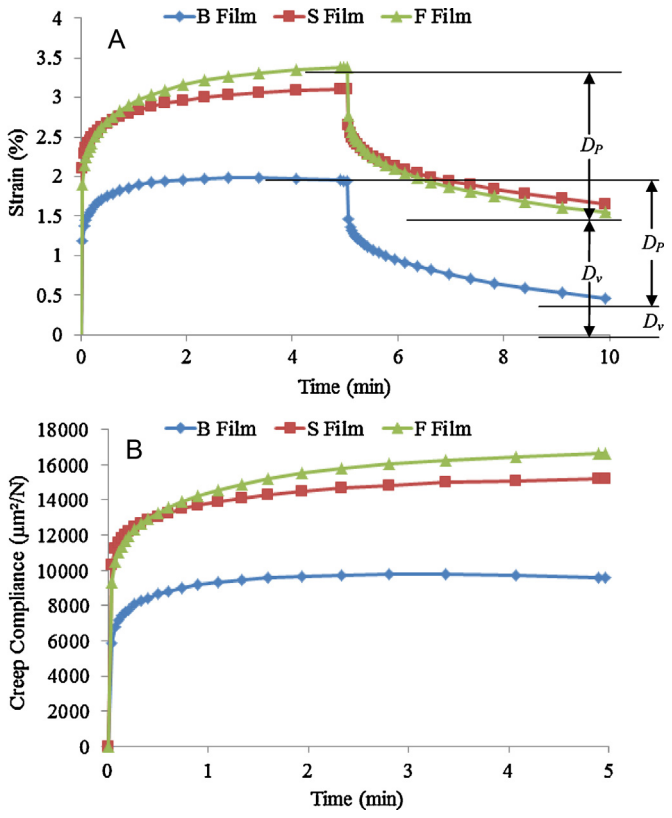

Fig. 3. Creep-recovery versus time of starch films in the absence and presence of starch nanoparticles. Panel A represents the creep-recovery curves and panel B represents the creep compliance versus time curves.

the presence of starch nanoparticles increases the magnitude of both the elastic and viscous components of starch films. From Fig. 2, the values of elastic modulus were larger than that of viscous modulus which could illustrate the dominant of elastic deformation in starch films with starch nanoparticles. At the same creep stress, starch films containing starch nanoparticles showed higher elastic deformation than the control film. The loss of viscous modulus during the deformation period is much higher in starch films containing starch nanoparticles compared to the starch-only (control) film. This fact explains the observation that in the recovery stage, starch films containing starch nanoparticles show higher plastic deformation (D_p) as well as viscous deformation (D_v) as shown in Fig. 3. The starch film containing vacuum freeze dried starch nanoparticles exhibits higher stable strain (the end of creep process) than the film containing spray dried starch nanoparticles. Fig. 3B shows the creep compliance data of starch films in the absence and presence of starch nanoparticles. It can be seen from this figure that in creep stage, all of these films can achieve stable creep compliance values and that the presence of starch nanoparticles increases the magnitude of creep compliance data. In addition, the starch film containing the vacuum freeze dried starch nanoparticles shows higher magnitude of stable creep compliance data compared to the film containing spray dried starch nanoparticles just as was observed in creep and recovery behavior (Fig. 3A).

The 3-parameter Burger's model [Eq. (4)] was used to predict the creep recovery behavior of these films (van der Vegt, 2006, Chapter 6). In Eq. (4), the first term is a constant and does not change with time; the second term represents the early stage of creep, but reaches the highest strain value very fast. The third term represents the trend in the creep behavior in a sufficiently long time.

$$\varepsilon = \frac{\sigma_0}{E_M} + \frac{\sigma_0}{E_K}\left(1 - e^{-t/\tau}\right) + \frac{\sigma_0}{\eta_M} \times t \qquad (4)$$

Here, ε represents the strain (%) of suspension, t represents the time (s) after loading. σ_0 represents the stress loaded (MPa), E_M and η_M are the modulus (MPa) and viscosity (MPa s) of the Maxwell spring and dashpot, respectively. Similarly, E_K and η_K are the modulus (MPa) and viscosity (MPa s) of the Kelvin spring and dashpot, respectively. Similarly, $\tau = \eta_K/E_K$ is the time taken to recover 63.2% or $(1 - e^{-1})$ of the total deformation in the Kelvin unit. The parameters E_M, E_K, η_M, and τ were obtained from fitting the experimental data to Eq. (4) with SPSS 16.0 (SPSS Inc., Chicago, USA).

Table 2 presents the values of the above mentioned four parameters for test films. As can be seen from this table, the Burger's model fits the experimental strain versus time data reasonably well ($R^2 > 0.96$). Specifically, starch film containing spray dried starch nanoparticles shows the highest E_M value while other two films exhibit relatively lower E_M values. The time independent term in Eq. (4) represents the instantaneous elastic deformation (σ_0/E_M) (Wang & Zhao, 2008). As the value of E_M (over 10^6 MPa) is much higher than the loaded stress (2 MPa), the data presented in Table 2 indicate that the starch films with and without starch nanoparticles have negligible instantaneous deformation.

The starch films containing starch nanoparticles show lower E_K values than the control film (Table 2). The films containing spray dried and vacuum freeze dried starch nanoparticles have almost similar E_K values ($P > 0.05$). All of these films show almost similar retardation time (τ) values ($P > 0.05$). In addition, starch-only film showed the highest η_M value while the film containing vacuum freeze dried starch nanoparticles have the lowest η_M value. Here, E_K and η_K ($\tau = \eta_K/E_K$) are associated with the stiffness and viscous or flow orientation of amorphous polymer chains in short time frame (Wang & Zhao, 2008). Hence, during the creep-recovery phase, the presence of starch nanoparticles enhances the orientation of amorphous chains including elastic deformation and viscous flow which results into lower E_K and η_K and lower recovery rate as shown in Table 2. However, the close τ values in these films suggest that the rate of decrease of E_K and η_K is almost the same. Besides, the permanent viscous flow parameter η_M indicates that the creep behavior in the second creep stage might be due to the damage in the crystalline structure of the polymer or damage in the structural orientation of the non-crystalline regions and the irreversible deformation in amorphous regions (Wang & Zhao, 2008). The presence of starch nanoparticles seemingly decreases such effect and this can explain why the decrease in the η_M value has occurred.

Based on the Burger's model, the creep rate (ε') can be calculated by using Eq. (5) which was the derivative of Eq. (4) ($\tau = \eta_K/E_K$) (Wang & Zhao, 2008).

$$\varepsilon'(t) = \frac{d\varepsilon(t)}{dt} = \frac{\sigma_0}{\eta_K} \cdot e^{-t/\tau} + \frac{\sigma_0}{\eta_M} \quad (5)$$

The creep rate will asymptotically reach a constant value in the stable creep stage ($t = \infty$) as shown in Eq. (6).

$$\varepsilon'(\infty) = \left.\frac{d\varepsilon(t)}{dt}\right|_{t=\infty} = \frac{\sigma_0}{\eta_M} \quad (6)$$

The $\varepsilon'(\infty)$ for these three films are presented in Table 2. As can be seen from this table the final creep rate $\varepsilon'(\infty)$ is increased significantly when the starch nanoparticles are incorporated in the starch films which also reflect on the changes occurring in the internal structure of starch film due to the presence of nanoparticles.

3.4. Analysis of time–temperature superposition (TTS)

The creep behavior (strain *versus* time) of the test films at different temperatures is presented in Fig. 4 using a logarithmic scale. This figure shows that the creep strain decreases with the increase in temperature (30–90 °C) in all these starch films. It can also be seen from Fig. 4 that the presence of starch nanoparticles more

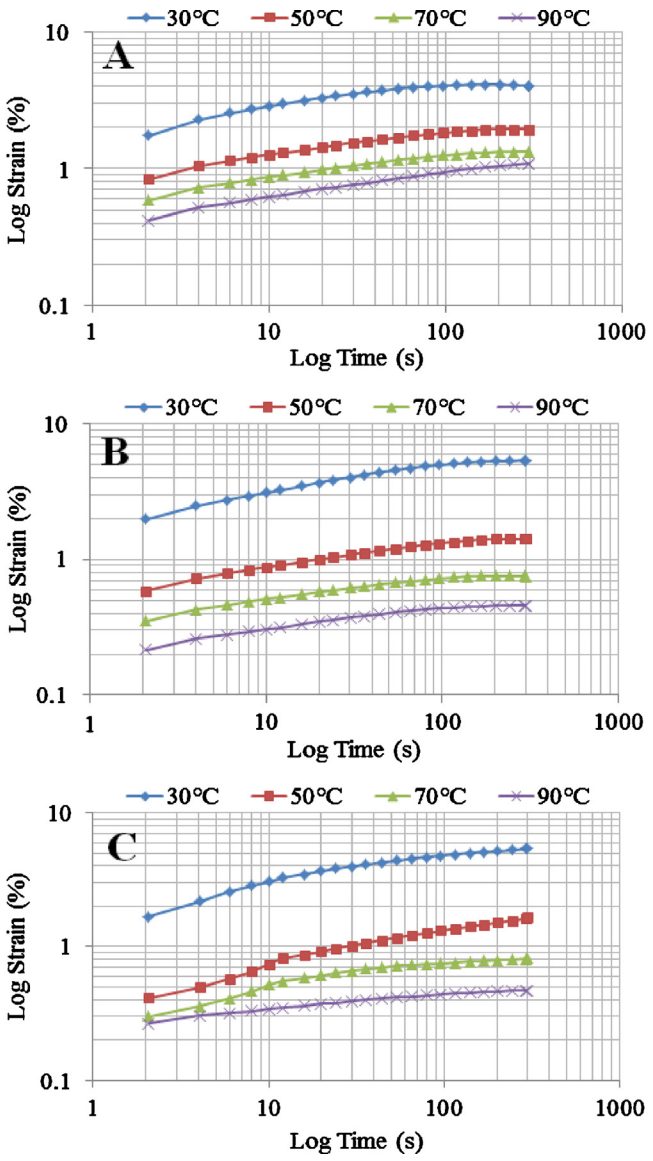

Fig. 4. The variation of creep strain with time presented in logarithmic scale in the presence and absence of starch nanoparticles different temperatures. Panel A represents B film; panel B represents S film; and panel C represents F film.

effectively reduces the creep strain of the films. This observation suggests that the presence of starch nanoparticles enhances the temperature sensitivity of starch films (Martucci, Ruseckaite, & Vázquez, 2006).

Fig. 5A presents the TTS master curves for a 20 day period based on the shift factor presented in Fig. 5B. These master curves were constructed using 90 °C as reference temperature. As can be seen from Fig. 5A, the starch films in the absence of starch nanoparticles show the lowest creep resistance. This figure shows that the presence of starch nanoparticles enhances the creep resistance of the starch films. It can further be seen from Fig. 5A that the there is significant difference in the creep resistance between the films containing spray dried and vacuum freeze dried starch nanoparticles in a longer time frame. The control starch film exhibits the lowest creep rate which is due to the fact that the films containing starch nanoparticles had higher temperature sensitivity (Xu, 2009).

The temperature dependence of the shift factors is represented well by the Arrhenius equation [Eq. (1)] with $R^2 > 0.97$ as shown in Fig. 5B. The calculated activation energy (E_a) values for these starch

Table 2
Burger's modeling parameters of creep-recovery behavior of starch films in the absence and presence of starch nanoparticles.[f]

Film type	E_M ($\times 10^6$ MPa)	E_K (MPa)	τ (s)	η_M (MPa s)	R^2	$\dot{\varepsilon}$ (∞) ($\times 10^{-3}$ s^{-1})	Recovery rate (%)
B Film	8.58 ± 1.822[a]	1.171 ± 0.056[a]	2.490 ± 0.340[a]	1672.098 ± 365.010[a]	0.965	1.196	76.57
S Film	86.578 ± 3.236[b]	0.776 ± 0.012[b]	1.576 ± 0.263[a]	904.403 ± 118.420[b]	0.980	2.211	46.68
F Film	15.413 ± 8.749[a]	0.775 ± 0.042[b]	2.211 ± 0.329[a]	598.653 ± 71.938[c]	0.969	3.341	54.55

[f] Values represent the mean ± standard deviation of triplicate tests. Values in a column with different superscripts were significantly different ($p < 0.05$).

films are summarized in Table 3. As can be seen from this table, the presence of starch nanoparticles has significantly ($P < 0.05$) increased the activation energy of the films. Specifically, the starch film with spray dried starch nanoparticles has the highest value of activation energy (81.745 kJ/mol) while the control sample has the lowest one (62.960 kJ/mol). This can be attributed to the fact that higher energy was required to increase the mobility of the starch molecules in films containing starch nanoparticles (Yang, Zhang, Schlarb, & Friedrich, 2006). The higher elastic and viscous modulus values in the films containing starch nanoparticles (Fig. 2) can be another reason that would consume more energy during creep tests.

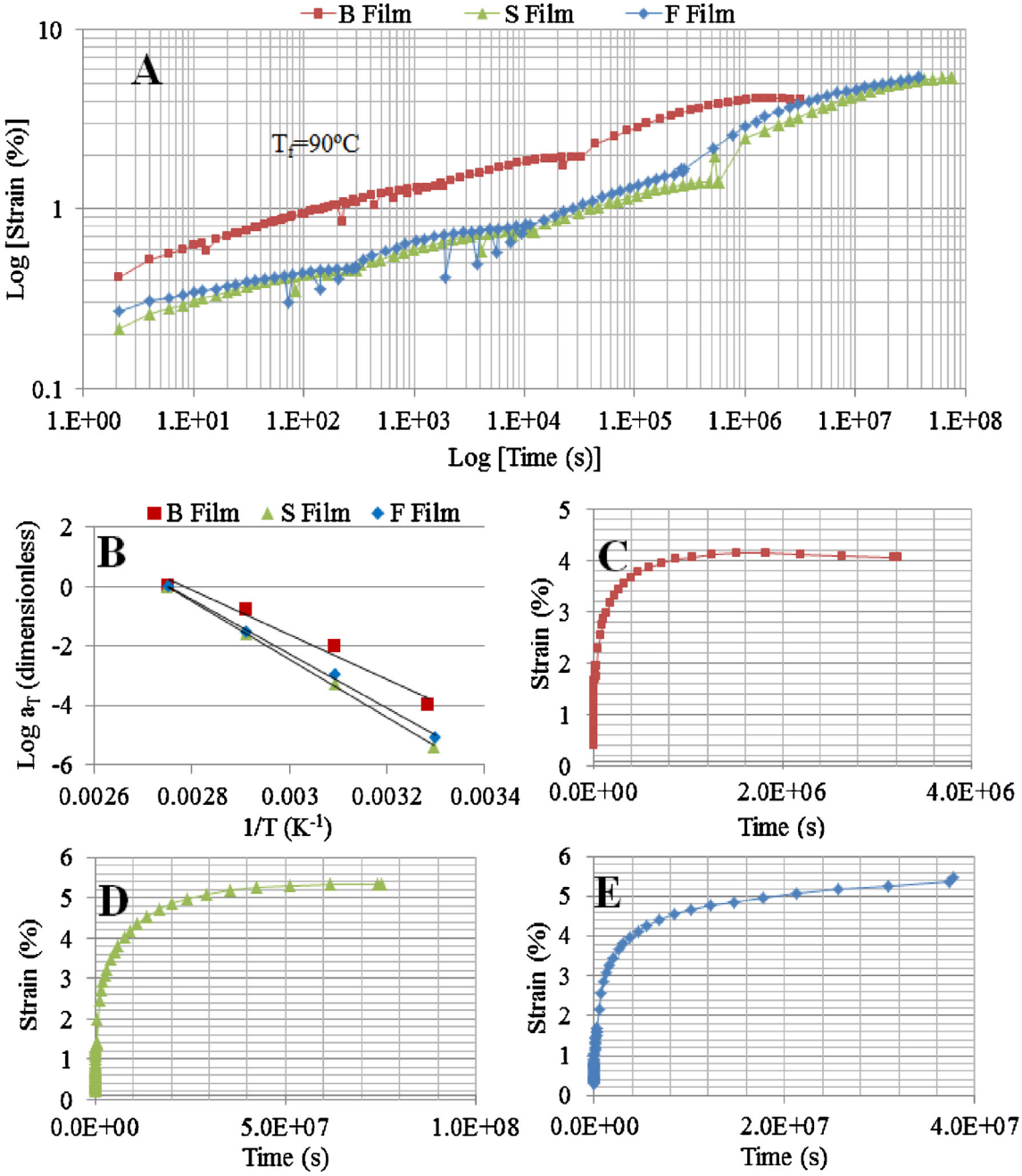

Fig. 5. The time temperature superimposition (TTS) master curves of creep, shift factor and TTS predicted creep behavior (over 20 days) for the starch films in the absence and presence of starch nanoparticles. Panel A: TTS master curves for all films; panel B: temperature dependence of shift factor (Arrhenius equation); panels C–E: TTS predicted creep for B film, S film and F film.

Table 3
The activation energy (E_a) values calculated using Arrhenius equation for starch films in the absence and presence of starch nanoparticles.[f]

Film type	E_a (kJ/mol)	R^2
B Film	62.960 ± 0.503[a]	0.973
S Film	81.745 ± 0.037[b]	0.999
F Film	76.486 ± 0.031[c]	0.996

[f] Values represent the mean ± standard deviation of triplicate tests. Values in a column with different superscripts were significantly different ($p < 0.05$).

Finally, the TTS predicted creep strain values of all the tested films for a duration of over 20 days at 90 °C are presented in Fig. 5C–E. It can be seen from this figure that the TTS method shows that the films containing starch nanoparticles allow prediction of creep behavior a longer period (around 10^7 s) than the starch only control films (around 10^6 s). At the longer time frame, both the trend and magnitude ($P > 0.05$) of creep strain of the films containing both types of starch nanoparticles are similar. Fig. 5C–E further illustrates the effect of starch nanoparticles on the internal structure of starch film containing such particles.

4. Conclusions

The frequency sweep and creep behavior of starch film with and without starch nanoparticles were investigated. The results from frequency sweep tests showed that the starch-only film exhibited dominant elastic behavior (than viscous behavior) while the presence of starch nanoparticles increased the storage modulus, loss modulus and tan δ quite significantly ($p < 0.05$) over the entire frequency range studied (0.1–100 rad/s). Power law model was found to basically fit the frequency dependence of elastic and viscous modulus ($R^2 > 0.79$). The presence of the starch nanoparticles affected the Power law parameters significantly. The incorporation of starch nanoparticles in starch film was found to significantly increase the creep strain, creep compliance and creep rate at long time frame. The effect of spray and vacuum freeze dried starch nanoparticles on the creep strain, creep compliance and creep rate at long time frame was not different statistically. The Burgers model predicted the experimental creep data reasonably well ($R^2 > 0.96$). The parameters of the Burger model were also affected by the addition of starch nanoparticles. The rate of creep recovery of starch film was reduced due to the presence of starch nanoparticles. The TTS method was successfully used to predict the creep behavior of these films for longer time frame (over 20 days). The temperature dependence of shift factor was successfully predicted using Arrhenius equation. The TTS master curves (for over 20 days) showed that the incorporation of starch nanoparticles increased the activation energy of the starch films and made the film less sensitive to the temperature. The TTS master curves of the films containing spray dried and vacuum freeze dried starch nanoparticles were similar both in magnitude and the trend.

Acknowledgments

This research was supported by National Natural Science Foundation of China (31000813), Chinese Universities Scientific Fund (2012QJ009), High Technology Research and Development Program of China (2011AA100802), Commonweal Guild Agricultural Scientific Research Program of China (201003077), and Science and Technology Program of Beijing (D12110003112002).

References

Alvarez, V. A., Kenny, J. M., & Vázquez, A. (2004). Creep behavior of biocomposites based on sisal fiber reinforced cellulose derivatives/starch blends. *Polymer Composites*, *25*(3), 280–288.

Alves, V. D., Mali, S., Beléia, A., & Grossmann, M. V. E. (2007). Effect of glycerol and amylose enrichment on cassava starchfilm properties. *Journal of Food Engineering*, *78*(3), 941–946.

Avella, M., De Vlieger, J. J., Errico, M. E., Fischer, S., Vacca, P., & Volpe, M. G. (2005). Biodegradable starch/clay nanocomposite films for food packaging applications. *Food Chemistry*, *93*, 467–474.

Bonacucina, G., Martino, P. D., Piombetti, M., Colombo, A., Roversi, F., & Palmieri, G. F. (2006). Effect of plasticizers on properties of pregelatinised starch acetate (Amprac 01) free films. *International Journal of Pharmaceutics*, *313*, 72–77.

Cespi, M., Bonacucina, G., Mencarelli, G., Casettari, L., & Palmieri, G. F. (2011). Dynamic mechanical thermal analysis of hypromellose 2910 free films. *European Journal of Pharmaceutics and Biopharmaceutics*, *79*(2), 458–463.

Chen, C.-H., & Lai, L.-S. (2008). Mechanical and water vapor barrier properties of tapioca starch/decolorized Hsian-Tsao leaf gum films in the presence of plasticizer. *Food Hydrocolloids*, *22*(8), 1584–1595.

Chevali, V. S., Dean, D. R., & Janowski, G. M. (2010). Effect of environmental weathering on flexural creep behavior of long fiber-reinforced thermoplastic composites. *Polymer Degradation and Stability*, *95*(12), 2628–2640.

Dawson, P. L., Hirt, D. E., Rieck, J. R., Acton, J. C., & Sotthibandhu, A. (2003). Nisin release from films is affected by both protein type and film-forming method. *Food Research International*, *36*(9–10), 959–968.

Famá, L., Rojas, A. M., Goyanes, S., & Gerschenson, L. (2005). Mechanical properties of tapioca-starch edible films containing sorbates. *LWT: Food Science and Technology*, *38*(6), 631–639.

Fu, Z-q., Wang, L-j., Li, D., Wei, Q., & Adhikari, B. (2011). Effects of high-pressure homogenization on the properties of starch-plasticizer dispersions and their films. *Carbohydrate Polymers*, *86*(1), 202–207.

Kampeerapappun, P., Aht-ong, D., Pentrakoon, D., & Srikulkit, K. (2007). Preparation of cassava starch/montmorillonite composite film. *Carbohydrate Polymers*, *67*, 155–163.

Kim, S. Y., Kim, S. H., Oh, H. J., Lee, S. H., Baek, S. J., Youn, J. R., et al. (2009). Molded geometry and viscoelastic behavior of film insert molded parts. *Journal of Applied Polymer Science*, *111*(2), 642–650.

Krogars, K., Heinämäki, J., Antikainen, O., Karjalainen, M., & Yliruusi, J. (2003). A novel amylose corn-starch dispersion as an aqueous film coating for tablets. *Pharmaceutical Development and Technology*, *8*(3), 211–217.

Laohakunjit, N., & Noomhorm, A. (2004). Effect of plasticizers on mechanical and barrier properties of rice starch film. *Starch/Stärke*, *56*(8), 348–356.

Martucci, J. F., Ruseckaite, R. A., & Vázquez, A. (2006). Creep of glutaraldehyde-crosslinked gelatin films. *Materials Science and Engineering A*, *435–436*, 681–686.

Mendieta-Taboada, O., Sobral, P. J. A., Carvalho, R. A., & Habitante, A. M. B. Q. (2008). Thermomechanical properties of biodegradable films based on blends of gelatin and poly(vinyl alcohol). *Food Hydrocolloids*, *22*(8), 1485–1492.

Muscat, D., Adhikari, B., Adhikari, R., & Chaudhary, D. S. (2012). Comparative study of film forming behaviour of low and high amylose starches using glycerol and xylitol as plasticizers. *Journal of Food Engineering*, *109*(2), 189–201.

Obara, S., & McGinity, J. W. (1994). Preparation and evaluation of diltiazem hydrochloride diffusion-controlled transdermal delivery system. *Pharmaceutical Research*, *11*(11), 1562–1567.

Patra, N., Salerno, M., Diaspro, A., & Athanassiou, A. (2011). Study of dynamic viscoelastic behavior of polystyrene films on addition of oleic acid. *Microelectronic Engineering*, *88*, 1849–1851.

Ryu, S. Y., Rhim, J. W., Roh, H. J., & Kim, S. S. (2002). Preparation and physical properties of zein-coated high-amylose corn starch film. *Lebensmittel-Wissenschaft und-Technologie*, *35*, 680–686.

Shaito, A. A. (2008). *Long term property prediction of polyethylene nanocomposites*. Ph.D. thesis. University of North Texas.

Shi, A-m., Li, D., Wang, L-j., Li, B-z., & Adhikari, B. (2011). Preparation of starch-based nanoparticles through high-pressure homogenization and miniemulsion cross-linking: Influence of various process parameters on particle size and stability. *Carbohydrate Polymers*, *83*(4), 1604–1610.

Talja, R. A. (2007). *Preparation and characterization of potato starch films plasticized with polyols*. Ph.D. thesis. Department of Food Technology, University of Helsinki.

Tselev, A., Brooks, C. M., Anlage, S. M., Zheng, H., Salamanca-Riba, L., Ramesh, R., et al. (2004). Evidence for power-law frequency dependence of intrinsic dielectric response in the $CaCu_3Ti_4O_{12}$. *Physical Review B*, *70*, 144101 (8 pp).

Urzhumtsev, Y. S. (1975). Time–temperature superposition. Review. *Mechanics of Composite Materials*, *11*, 57–72.

van der Vegt, A. K. (2006). Visco-elasticity from polymers to plastics. *VSSD*, 115–132.

Veiga-Santos, P., Oliveira, L. M., Cereda, M. P., & Scamparini, A. R. P. (2007). Sucrose and inverted sugar as plasticizer: Effect on cassava starch-gelatin film mechanical properties, hydrophilicity and water activity. *Food Chemistry*, *103*(2), 255–262.

Wang, Z. D., & Zhao, X. X. (2008). Modeling and characterization of viscoelasticity of PI/SiO_2 nanocomposite films under constant and fatigue loading. *Materials Science and Engineering A*, *486*, 517–527.

Weick, B. L. (2006). Viscoelastic analysis applied to the determination of long-term creep behavior for magnetic tape materials. *Journal of Applied Polymer Science*, *102*(2), 1106–1128.

Wittaya, T. (2009). Microcomposites of rice starch film reinforced with microcrystalline cellulose from palm pressed fiber. *International Food Research Journal*, *16*, 493–500.

Wu, M., Wang, M., & Ge, M-q. (2009). Investigation into the performance and mechanism of SiO_2 nanoparticles and starch composite films. *Journal of the Textile Institute*, *100*(3), 254–259.

Xu, Y.-j. (2009). *Creep behavior of natural fiber reinforced polymer composites*. Ph.D. thesis. The School of Renewable Natural Resources, Louisiana State University.

Xu, Y.-j., Wu, Q.-l., Lei, Y., & Yao, F. (2010). Creep behavior of bagasse fiber reinforced polymer composites. *Bioresource Technology*, *101*(9), 3280–3286.

Xu, Y. X., Kim, K. M., Hanna, M. A., & Nag, D. (2005). Chitosan–starch composite film: Preparation and characterization. *Industrial Crops and Products*, *21*(2), 185–192.

Yang, J.-l., Zhang, Z., Schlarb, A. K., & Friedrich, K. (2006). On the characterization of tensile creep resistance of polyamide 66 nanocomposites. Part II: Modeling and prediction of long-term performance. *Polymer*, *47*, 6745–6758.